Integrating Cell Phone Imaging with Magnetic Levitation (i-LEV) for Label-Free Blood Analysis at the Point-of-Living

*Murat Baday, Semih Calamak, Naside Gozde Durmus, Ronald W. Davis, Lars M. Steinmetz, and Utkan Demirci**

There is an emerging need for portable, robust, inexpensive, and easy-to-use disease diagnosis and prognosis monitoring platforms to share health information at the point-of-living, including clinical and home settings. Recent advances in digital health technologies have improved early diagnosis, drug treatment, and personalized medicine. Smartphones with high-resolution cameras and high data processing power enable intriguing biomedical applications when integrated with diagnostic devices. Further, these devices have immense potential to contribute to public health in resource-limited settings where there is a particular need for portable, rapid, label-free, easy-to-use, and affordable biomedical devices to diagnose and continuously monitor patients for precision medicine, especially those suffering from rare diseases, such as sickle cell anemia, thalassemia, and chronic fatigue syndrome. Here, a magnetic levitation-based diagnosis system is presented in which different cell types (i.e., white and red blood cells) are levitated in a magnetic gradient and separated due to their unique densities. Moreover, an easy-to-use, smartphone incorporated levitation system for cell analysis is introduced. Using our portable imaging magnetic levitation (i-LEV) system, it is shown that white and red blood cells can be identified and cell numbers can be quantified without using any labels. In addition, cells levitated in i-LEV can be distinguished at single-cell resolution, potentially enabling diagnosis and monitoring, as well as clinical and research applications.

1. Introduction

Rapid diagnostic tools are used in multiple fields, including clinical and veterinary medicine, as well as food safety.[1–7] Point-of-care (POC) devices enable inexpensive, rapid, portable, label-free, accessible, and easy-to-use diagnostic solutions.[8–12] Moreover, POC devices can be applied to monitor compliance and disease progression.[13] However, most systems require extensive sample preparation and labeling

Dr. M. Baday, S. Calamak, Prof. U. Demirci
Canary Center at Stanford for Cancer Early Detection
Radiology Department
School of Medicine
Stanford University
CA 94304, USA
E-mail: utkan@stanford.edu
Dr. N. G. Durmus, Prof. R. W. Davis
Department of Biochemistry
School of Medicine
Stanford University
CA 94304, USA
Dr. N. G. Durmus, Prof. R. W. Davis,
Prof. L. M. Steinmetz
Stanford Genome Technology Center
Stanford University
CA 94304, USA
Prof. R. W. Davis, Prof. L. M. Steinmetz
Department of Genetics
School of Medicine
Stanford University
CA 94304, USA

DOI: 10.1002/smll.201501845

Table 1. Complete blood count methods.

Parameters	Hemocytometer[35]	Flow cytometer (FACS)[34,35]	Coulter counter[36]	Miniature microfluidic devices[37–39]	i-LEV
Functionality	Hemocytometers are cell-counting devices consisting of a microfluidic channel with 100 μm depth. Images are taken with a conventional microscope	Flow cytometers are used for cell counting as well as cell sorting. Cells are suspended as they flow in a stream through a laser beam	A Coulter counter is designed for cell counting as the cells are suspended in electrolytes	Several of these devices are used for blood counting and separation in microfluidic systems, including electro-osmotic flow, bifurcation, geometric obstructions, acoustic standing wave forces, porous filters, membrane filtration and cross-flow filtration	i-LEV is used to asses blood counts. The width of the blood band across a capillary is measured to quantify the blood concentration.
Assay time	>20 min	>1 h	>1 h	>2 h	15 min stabilization time and less than 30 sec of analysis time
Labeling	Not required	Required	Not Required	Required	Not required
Cost	$10	Requires LASER detection system >$10.000	>$5.000	>$2.000	$1 for chambers
Complexity	Since cell counting is performed manually, it is time consuming. It is not as sensitive due to sampling errors	It requires high volume of blood. Reagents for pretreatment are expensive. Training required for laboratory technicians	Requires extensive design and circuit building. It must be calibrated regularly	Miniature microfluidic devices require an independent liquid flow source such as a peristaltic pump or a syringe pump, and cannot easily be produced in a portable platform	i-LEV consists of a magnetic levitation device and a smartphone. It requires a finger-prick volume of blood.
Accessibility	Deliverable and it can be used in centralized lab settings	Performed at established centers, hospitals and clinics	Generally performed at established hospitals and clinics	Deliverable and it can be used without requiring centralized hospitals or clinics	i-LEV can provide simple blood counting tests accessible to the general public in multiple settings, including home and clinical settings.

steps, which limit their usage. Precision medicine tailors treatments to a patient's profile based on their genetic data. Cellular and molecular analyses are increasingly being performed by research institutions and drug companies to achieve more efficient drug development and improved early diagnoses. In this respect, smartphones with high-resolution cameras, fast computing power, graphics processors, data storage, and connectivity capacities are used for various healthcare platforms, including telemedicine and POC diagnostics.[14–23] The red blood cell (RBC) and white blood cell (WBC) count is a crucial diagnostic parameter assessed in pathology laboratories.[24–33] Currently, hemocytometry, coulter counting, or flow-cytometry are the most widely used methods to count an classify blood cell.[34] In **Table 1**, we compare the i-LEV device to these established methods. Coulter and flow-cytometry are complex and expensive, whereas hemocytometry is inexpensive but labor intensive, time-consuming, and not practical for POC testing. Recently developed methods have advanced the field by applying sensitive and robust technologies. However, an inexpensive and accurate blood count analyzer is still missing for POC monitoring.

In recent years, magnetic levitation principles have been used to monitor and biologically characterize cells and cellular events.[40–45] Our earlier studies have shown that different cell types with various sizes ranging down to the sub-micron level can be aligned at unique heights using levitation platforms. Here, we present a smartphone-based magnetic levitation system to identify and quantify blood cells without using labels. Our system assesses RBC and WBC counts in whole blood samples by analyzing the width of the blood band in a high magnetic field. Previously, the separation of blood cells without labeling has posed a significant challenge in clinical diagnostics. Using our system, RBC and WBC can be separated due to their unique density signatures. The i-LEV device is an easy-to-use and easy-to-access POC solution for blood cell counting that could be used to monitor disease progression and drug effectiveness in the home-setting.

2. Results

Our portable, magnetic levitation-based imaging platform shown in Figure 5 has several components including: i) a front panel with several threads to mount components of the system; ii) a lens, which is placed right behind the smartphone to focus the images on the camera; iii) a levitation device with capillaries that is placed directly below the lens to image the band width of levitated blood cells, iv) additional components such as simple LED light sources and ND filters to improve the images. The front panel has a slide-in door to block external light. The set-up was designed using PMMA building blocks prepared with a laser cutter. The levitation device is made of magnets, mirrors, and channel. Two permanent magnets (50 mm length, 2 mm width, and 5 mm height) are set up in such an orientation that the same poles face each other. A capillary channel (50 mm length, 1 mm × 1 mm cross-section, 0.2 mm wall thickness) can be inserted between the magnets. Side mirrors are used to illuminate and observe the levitation channel. Samples spiked into a paramagnetic medium (i.e., Gadavist) are levitated inside the medium at a position where the buoyancy force and the magnetic force are equal. The levitation height of the sample is calculated based on Equation (1).

$$\frac{\Delta\chi}{\mu_0} B.\nabla B - \Delta\rho g = 0 \quad (1)$$

DOI: 10.1002/smll.201501845

small NANO MICRO

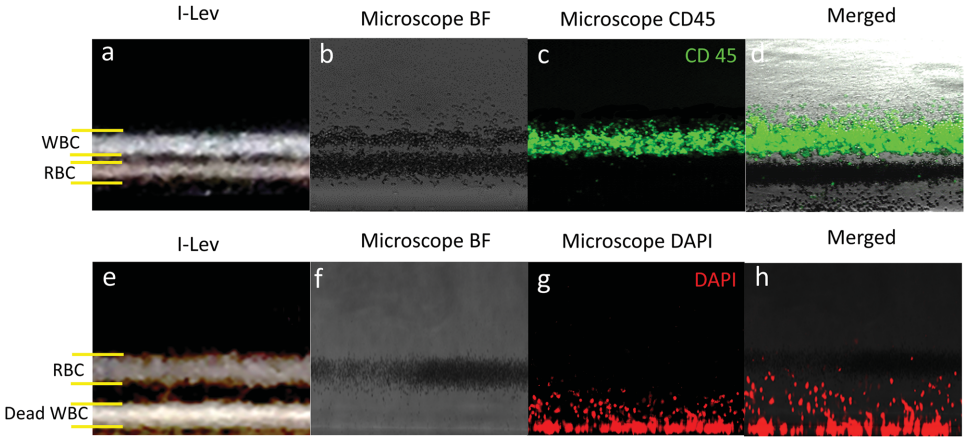

Figure 1. Separation of red and white blood cells within the i-LEV platform.a) WBC and RBC separation image taken by i-LEV. b) RBC and WBCs levitated at different heights are imaged by conventional microscopy using bright field. c) Fluorescent images of CD45-labeled WBC. d) Overlap of the bright field and CD45 images to confirm the separation of WBC and RBC. e) Live–dead assay imaging of RBCs and WBCs by i-LEV. Live RBCs levitate while dead WBCs aggregate at bottom of the capillaries. f) Bright field, g) DAPI labeled, and h) Overlapping images of WBC using fluorescence microscopy.

The first part of the equation represents the magnetic force applied to a particle, while the second part represents the buoyancy force. The magnetic induction, gravitational acceleration, difference between volumetric densities of cells and medium, and permeability of the free space are represented by B, g, ρ, and μ_0, respectively. Samples are levitated at unique heights mainly based on their density, independent of their mass and volume.[46,47] Therefore, only mass or only volume of the cells are not crucial for the levitation however, their unique densities determines the levitation height. Blood cells can be equilibrated in paramagnetic concentration lower than 100×10^{-3} M with the induction of magnetic gradient about 600 T m^{-1}.[48] Paramagnetic medium effects equilibration height as the more paramagnetic salt concentration increases the equilibration height. Cells with the same density as the paramagnetic medium are localized in the middle of the capillary channel, however cells with densities different from that of the medium are localized above or below the middle of the channel depends on their densities. To demonstrate the i-LEV system's potential to separate different sample species, RBC and WBC were mixed at equal concentrations of 5 million cells mL^{-1} and separated according to their different levitation characteristics (**Figure 1**a). The same samples were also imaged using regular microscopy to confirm the types of cells that levitated different heights (Figure 1b–d). Overlapped images of WBC labeled with CD45 and the bright-field image of the mixed RBC and WBC sample clearly validated the i-LEV results (Figure 1a–d). Additionally, we performed live–dead assays with WBC and RBC. First, WBC were stained and frozen overnight. These dead cells were then spiked into RBC samples at equal concentrations. The i-LEV system shows only RBC levitated at the middle of the channel, whereas dead WBC aggregated at the base (Figure 1e). To validate our results, we stained the dead WBC with DAPI and visualized them by fluorescence microscopy. The overlapped bright-field image of WBC (Figure 1f) and DAPI-stained WBC (Figure 1g) confirmed the dead–live assay results (Figure 1f–h).

Next, we levitated and separated a RBC and WBC mixture using two other Gadolinium (Gd^+) concentrations to identify the optimal Gd^+ concentration for cell separation experiments (Figure 1, Supporting Information). As we increased the Gd^+ concentration (e.g., 60×10^{-3} and 90×10^{-3} M), the levitation height rose and it became harder to distinguish the bands from one another. Our results indicate that the ideal Gd^+ concentration is around 30×10^{-3} M, as this concentration allows optimal levitation while keeping the cells at an adequate distance from the capillary walls. In this condition, the resulting bands are easy to distinguish.

We then used i-LEV to quantify RBC spiked in phosphate buffered saline (PBS). To evaluate equilibration time, we first performed calibration measurements at different time points. The whole blood samples spiked in PBS at a final concentration of 450 million cells mL^{-1} were levitated for 30 min. Samples were imaged every 3 min during levitation (Supplementary movie, Supporting Information), demonstrating that cells were equilibrated at their unique levitation heights after approximately 15 min (**Figure 2**a). Experiments with 90 million cells mL^{-1} blood were performed to test the stabilization time at different concentrations. The exponential time constants for the stabilization curves were 5.8 min for 450 million cells mL^{-1} and 3.3 min for 90 million cells mL^{-1}. The blood cell concentration versus time curves show that the equilibration time for the curves was again 15 min (Figure 2b). As expected, higher concentrations of blood cells took longer to equilibrate. Further validation experiments were performed to assess the changes in blood bandwidth at different concentrations. RBC were imaged with the i-LEV system at concentrations of 250, 125, 63, 50, 25, and 0.8 million cells mL^{-1}. Each sample was quantified using a hemocytometer to confirm the calculated blood counts. To assess the cell concentrations, the width of the levitated blood band across the channel was measured by dividing the total area of the blood by width of the illuminated region. At higher concentrations, between 50 and 250 million cells mL^{-1}, the blood width

DOI: 10.1002/smll.201501845

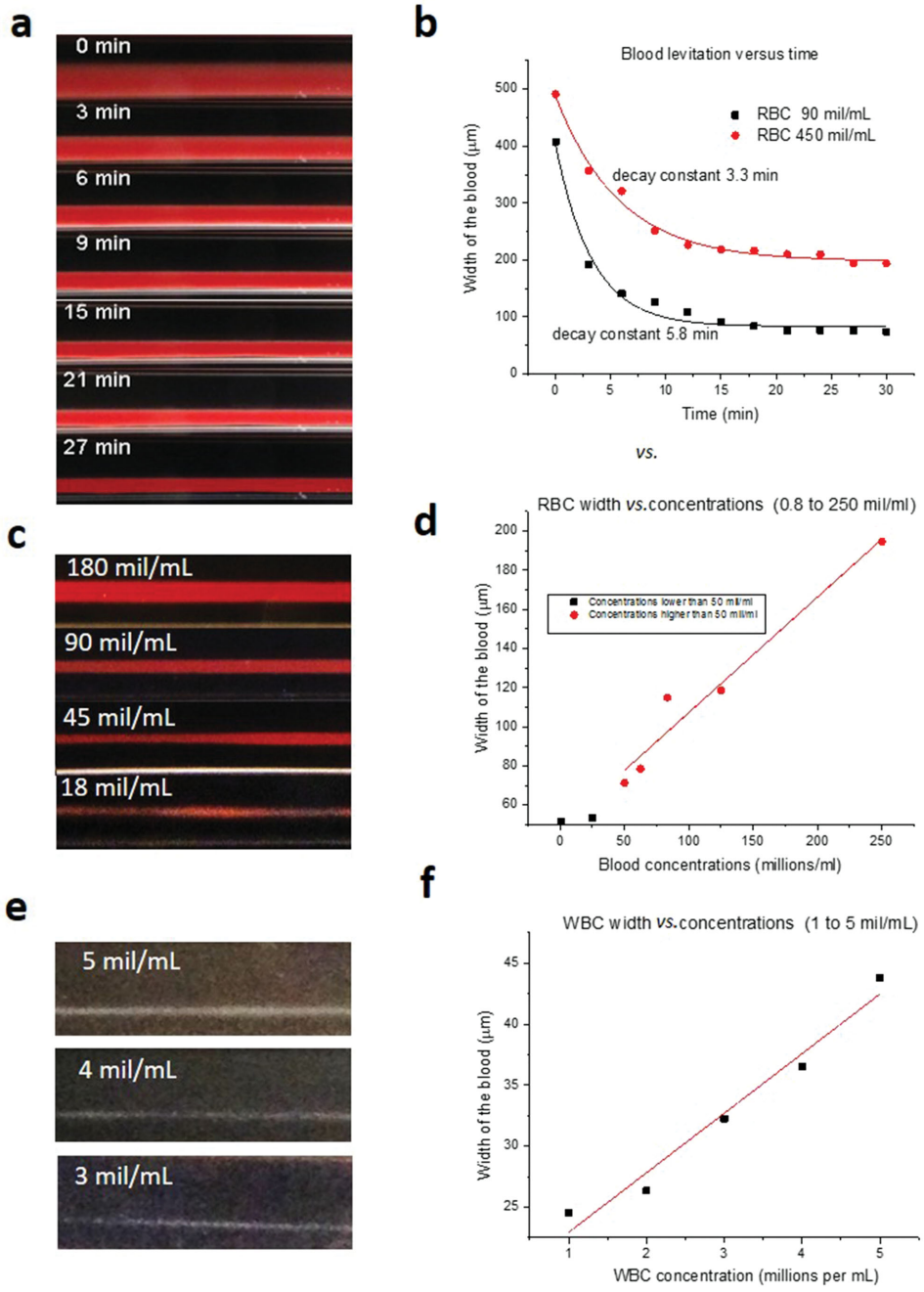

Figure 2. Width of the red and white blood cells at different dilutions and time points. a) Images of RBC band width at different time points show changes in width of the levitated cell bands over time. b) RBC with two different concentrations (90 and 450 million cells mL^{-1}) were analyzed by i-LEV for 30 min. c) Images of levitated red blood cells at different concentrations. d) The width of the blood band is plotted against the RBC concentration. RBC concentrations vary from 250 million cells mL^{-1} to 0.8 million cells mL^{-1}. The graph is linear within a cell concentration range between 50 and 250 million cells mL^{-1}. e) Images of levitated WBC at different concentrations. f) The width of the blood band is plotted against the WBC concentration.

versus concentrations curves were linear with a slope of 0.6 micrometers per million cells mL^{-1}. However, as the cell concentration decreased (i.e., 0.8 and 25 million cells mL^{-1}), the curves lost their linearity (Figure 2d). For blood cell concentrations above 50 million cells mL^{-1}, we observed that the width of the blood band during levitation was correlated with the cell concentration. We also imaged WBC at varying concentrations ranging from 1 to 5 million cells mL^{-1} and plotted the concentration against the width of the blood band (Figure 2e,f). WBC concentrations also correlated with the width of the blood band in a linear manner.

Using the i-LEV platform, we detected single cells without using any labels. After diluting the RBC concentration to 100.000 cells mL^{-1} or lower, we could quantify

small 2015,
DOI: 10.1002/smll.201501845

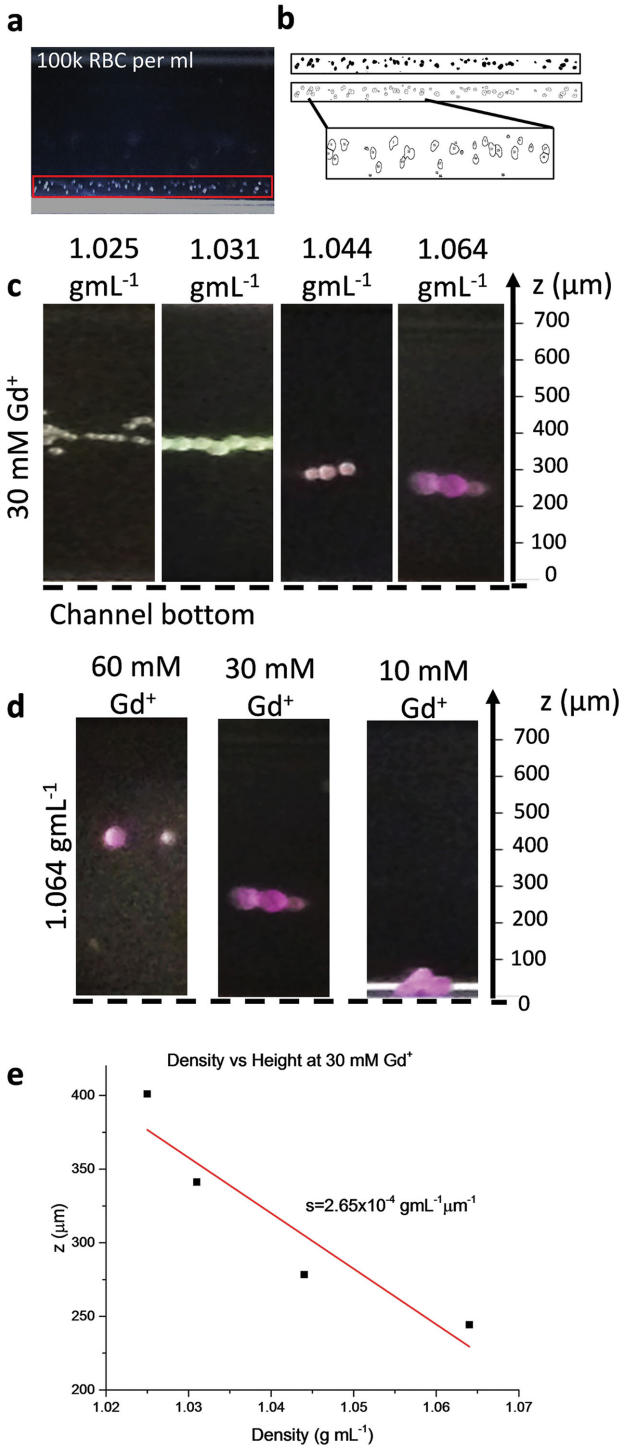

Figure 3. Single-cell detection and density measurements. a) Image of RBC at a concentration of 100.000 cells mL^{-1}. b) Single blood cells are detected using image algorithms. c) Density measurement of polyethylene beads in the magnetic levitation platform. Beads (10–100 µm in diameter) with different densities (1.025, 1.031, 1.044, 1.064 g mL^{-1}) have distinct levitation heights in 30×10^{-3} M Gd^+. d) Beads with 1.064 g mL^{-1} density had different levitation heights at different Gd^+ concentrations (10×10^{-3} M, 30×10^{-3} M, 60×10^{-3} M). e) Linear fitting curve provides a standard function to measure densities of particles.

individual cells in the illuminated area using simple image processing tools (**Figure 3**a,b). Finally, we levitated polyethylene beads in the capillaries to check the levitation resolution of the platform and show its potential to calculate densities for different samples and cells. Beads with various sizes between 10 and 100 µm in diameter with densities of 1.025, 1.031, 1.044, or 1.064 g mL^{-1} showed distinct levitation heights in 30×10^{-3} M Gd^+ (Figure 3c). We also observed that beads with 1.064 g mL^{-1} density had different levitation heights in different Gd^+ concentrations (10×10^{-3}, 30×10^{-3}, 60×10^{-3} M) (Figure 3d).

3. Discussion

Earlier studies have introduced several relevant biological applications for different magnetic levitation systems. Here, we present i-LEV, a novel platform combining magnetic levitation with a smartphone device. The i-LEV system reliably analyses blood cell counts and can also detect individual cells. It is a rapid, portable, easy to use, and affordable platform that leverages the availability of smartphones to address a medical need and count RBC as well as WBC from unprocessed whole blood. Today, blood processing is a clinical procedure and requires extensive materials and equipment, as well as trained professionals. Therefore, it can currently not be implemented in the POC setting. Our system could, however, enable blood analyses from home and facilitate disease diagnosis and monitoring.

The i-LEV device can also perform fluorescent imaging, as the set-up carries several slots to insert fluorescent LEDs, lenses, excitation filters, and emission filters (Figure 5c). Although, the current platform is static, it can be extended to enable dynamic flow experiments and monitor real-time effects of drugs on certain cell types that have been separated within capillaries. Using various microfluidics techniques combined with i-LEV system would provide environment for new applications such as studying effects of drugs on cells by monitoring in real time inside levitation channel as well as screening of circulating tumor cells. Customized smartphone apps for each application can improve the performance and high throughput of the i-LEV system that can give read-out right away after images acquired. Next-generation applications of the system may include advanced tests, for example, to monitor circulating blood cells or sickle cell disease, especially in resource-constrained settings. Levitation systems integrated into smartphones could provide simple blood tests for large populations as smartphones are extensively used across the world. It is estimated that globally, approximately 5 billion people use mobile phones.[49] In this respect, smartphone integrated medical technologies such as i-LEV could potentially play an important role in health services, particularly in developing countries with limited financial and logistical resources.

The i-LEV test results can be analyzed and evaluated using an app and can also be transferred to healthcare providers via integrated cloud platforms (**Figure 4**). The

DOI: 10.1002/smll.201501845

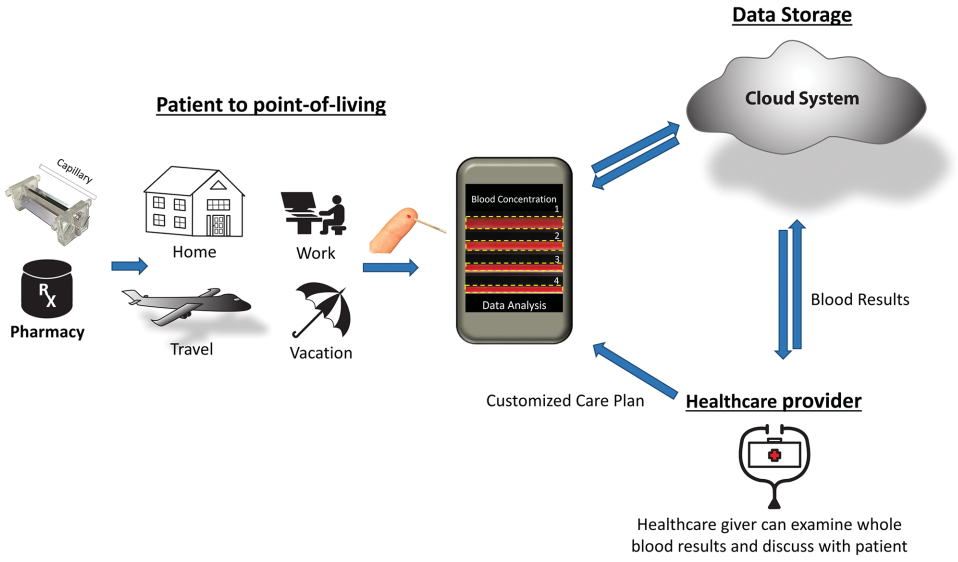

Figure 4. Diagram shows how i-LEV could be implemented and contributed to the healthcare system. Blood counting can be performed with an integrated mobile application at various settings (i.e., at home or work, or during travel or vacation). The mobile application reports the measurements to the healthcare provider. The healthcare provider analyzes the results and provides feedback through an online system.

portability, affordability, and simplicity of our platform result in an easy-to-use set-up for blood counting in home settings, as well as biological or clinical laboratories.

In the future, we plan to apply our technology to address further medically relevant questions using a POC approach to diagnose and monitor diseases. For example, we have previously shown that cells infected by viruses have distinct levitation characteristics, representing another promising application for the i-LEV system once again particularly relevant for developing countries.

4. Experimental Section

Experimental Setup: 3 mm thick poly(methyl methacrylate) (PMMA) pieces cut with a laser cutter (VLS 2.30 Versa Laser) were used to assemble the i-LEV system with dimensions of 160, 100, 205 mm, as shown in **Figure 5c**. Threads with 3 mm steps were designed to accommodate insertion parts for different applications. The top layer of the i-LEV system has several different versions that are compatible with different brands of smartphones. The height of the set-up can be halved for simple experiments, which do not require extensive optical systems and light sources. The full-size i-LEV system can accommodate fluorescent imaging hardware by inserting broadband LEDs, as well as excitation and emission filters. Microcapillary channel (1 mm × 1 mm cross-section, 50 mm length, and 0.2 mm wall thickness), N52 grade neodymium magnets (NdFeB) (50 mm length, 2 mm width, and 5 mm height), and side mirrors were used to build the magnetic levitation device (Figure 5a).

The levitation device was placed 3 cm below the smartphone that contained a lens adapter. Phones with auto-focus features can adjust the focal plane without having to move the sample up and down. Before each separate measurement, a microcapillary channel was placed between the magnets after the plasma had been treated for 3 min at 100 W, 0.5 Torr. Two mirrors were placed at 45° to pass the light through the levitation channel, as the magnets block the direct incoming light. The channel illumination is aligned with the smartphone camera.

Sample Measurements: RBC, WBC, and polyethylene beads were spiked in PBS containing different concentration of paramagnetic medium (30×10^{-3} M, 60×10^{-3} M, and 90×10^{-3} M Gd^{+}). 30 µL of sample was pipetted into the microcapillaries and the channel was sealed with Critoseal. The samples were levitated for 30 min until they reached their equilibrium height within the system. Calibration measurements were performed to quantify stabilization time (Figure 3a,b). The width and height of the cells and beads were imaged and analyzed using imageJ.

Levitation of Red Blood Cells: Blood samples from healthy donors were received from Stanford University Blood Center. Whole blood was diluted at varying ratios in PBS containing 30×10^{-3} M Gd^{+}. Concentrations were described in the results. Concentrations of 450 and 90 million cells mL^{-1} of blood were used to measure blood stabilization time. Varying concentrations of blood, ranging from 250 to 0.8 million cells mL^{-1} were used to correlate the width of the blood band and cell concentrations.

Levitation of White Blood Cells: Whole blood was mixed with RBC lysis buffer at a 1:10 ratio. RBC were lysed after 5 min of incubation and the blood samples were suspended at 1.500 rpm for 3 min. The resulting WBC pellet was resuspended in PBS. Incremental concentrations between 1 and 5 million WBC mL^{-1} were used to correlate the width of the WBC levitation band with the cell concentrations.

Experiments with Live White Blood Cells: WBC were labeled with anti-CD45 antibody- conjugated FITC (1:20 BD Pharmingen) for 30 min. WBC were then washed twice with PBS and resuspended in PBS. At the end of this process, live WBC and 1.000× RBC were suspended (50:50) in PBS with 30×10^{-3} M Gd^{+} at 1.500 rpm for 3 min. Cells were levitated for 30 min and imaged.

Experiments with Dead White Blood Cells: After RBC lysis, WBC were frozen overnight at −80 °C in PBS without a

DOI: 10.1002/smll.201501845

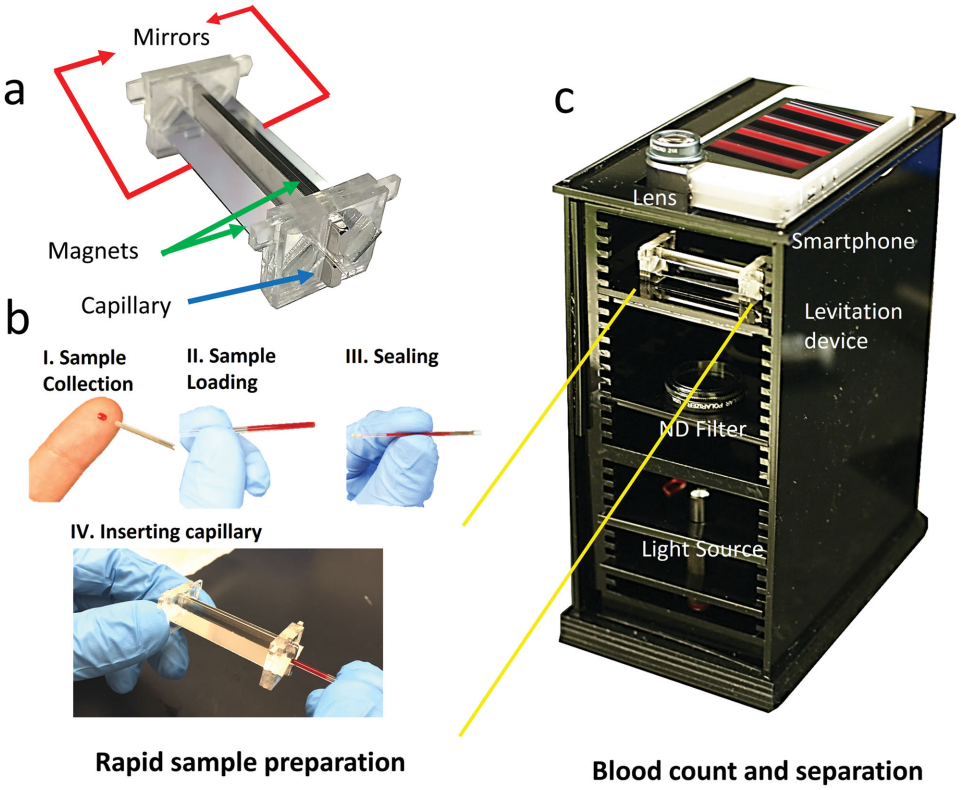

Figure 5. i-LEV platform for cell quantification and rapid sample preparation. a) Magnetic leviation device which is made of microcapillary channel, magnets and side mirrors. b-I) A small volume (30 µL) of a blood sample is loaded into the microcapillary, II) The blood sample is loaded to the microcapillary channel using capillary forces, III) The microcapillary channel is then sealed with Critoseal, IV) The capillary channel is introduced between two permanent neodymium magnets whose same poles are facing each other. c) The i-LEV set-up includes a smartphone, lens, levitation device, light source, and filters.

cryoprotective agent in order to kill WBC. After overnight incubation, dead WBC cells were stained with 4′,6-diamidino-2 phenylindole dihydrochloride (DAPI) (1:1.000 Invitrogen) for 15 min at room temperature. After staining, dead WBC were washed twice with PBS and resuspended in PBS. Finally dead WBC and 1.000× RBC were mixed and suspended (50:50) in PBS with 30×10^{-3} M Gd^{+} at 1500 rpm for 3 min. Cells were levitated for 30 min and imaged.

Image Analysis: Step-by-step image analysis of RBC was performed using ImageJ. Briefly, the image taken by the smartphone was uploaded to ImageJ. Then, the levitated blood band was cropped and the background was subtracted. The image was converted to 16-bit and the threshold was adjusted to "Default-BW" settings. Area, center of mass, and bounding rectangle were measured. Dividing the measured area by the bounding rectangle provided the average height of the blood band. Each step of image analysis is explained in more detail in the Supporting Information.

Supporting Information

Supporting Information is available from the Wiley Online Library or from the author.

Acknowledgements

M.B. and S.C. contributed equally to this work. The authors thank Allan Jones for his feedback during the preparation of this manuscript. The authors also thank Dr. H Cumhur Tekin for his help with simulations of the magnetic levitation system. U.D. acknowledges that this material is based in part upon work supported by the NSF CAREER Award Number 1150733, NIH R01EB015776-01A1, R21TW009915, and NIH R21HL112114. L.M.S. and R.W.D. acknowledge that this material is based in part upon work supported by NIH P01 HG000205. U.D. is a founder of, and has an equity interest in: (i) DxNow Inc., a company that is developing microfluidic and imaging technologies for point-of-care diagnostic solutions, and (ii) Koek Biotech, a company that is developing microfluidic IVF technologies for clinical solutions. UD's interests were reviewed and are managed by the Brigham and Women's Hospital and Partners HealthCare in accordance with their conflict of interest policies. We also thank The Scientific and Technical Research Council of Turkey (TUBITAK) for providing financial support (2214A-Abroad research support for Ph.D.students) to S.C. during his visit to BAMM Labs.

[1] A. K. Yetisen, M. S. Akram, C. R. Lowe, *Lab Chip* **2013**, *13*, 2210.
[2] H. Shafiee, W. Asghar, F. Inci, M. Yuksekkaya, M. Jahangir, M. H. Zhang, N. G. Durmus, U. A. Gurkan, D. R. Kuritzkes, U. Demirci, *Sci. Rep.* **2015**, *5*, 8719.

DOI: 10.1002/smll.201501845

[3] F. Inci, O. Tokel, S. Wang, U. A. Gurkan, S. Tasoglu, D. R. Kuritzkes, U. Demirci, *ACS Nano* **2013**, *7*, 4733.
[4] H. Shafiee, M. B. Sano, E. A. Henslee, J. L. Caldwell, R. V. Davalos, *Lab Chip* **2010**, *10*, 438.
[5] U. H. Yildiz, F. Inci, S. Q. Wang, M. Toy, H. C. Tekin, A. Javaid, D. T.-Y. Lau, U. Demirci, *Biotechnology Advances* **2015**, *33*, 178–190.
[6] S. Tasoglu, H. C. Tekin, F. Inci, S. Knowlton, S. Q. Wang, F. Wang-Johanning, G. Johanning, D. Colevas, U. Demirci, Proc. IEEE 103 **2015**, *2*, 161–178.
[7] V. Sowmya, T. N. Narayan, K. Aran, K. D. Flink, J. Paredes, P. M. Ajayan, S. Filipek, *Materials Today* **2015**, doi:10.1016/j.mattod.2015.04.003.
[8] S. Park, Y. Zhang, S. Lin, T.-H. Wang, S. Yang, *Biotechnol. Adv.* **2011**, *29*, 830.
[9] G. M. Whitesides, *Lab Chip* **2013**, *13*, 11.
[10] B. Sanavio, S. Krol, *Front. Bioeng. Biotechnol.* **2015**, *3*, 20.
[11] F. Benkebil, C. Combescure, S. I. Anghel, B. Duvanel, M. G. Schäppi, *World J. Gastroenterol.* **2013**, *19*, 5111.
[12] O. Tokel, U. H. Yildiz, F. Inci, N. G. Durmus, O. O. Ekiz, B. Turker, C. Cetin, *Sci. Rep.* **2015**, doi:10.1038/srep09152.
[13] F. Inci, C. Filippini, M. Baday, M. O. Ozen, S. Calamak, N. G. Durmus, S. Wang, E. Hanhauser, K. S. Hobbs, F. Juillard, P. P. Kuang, M. L. Vetter, M. Carocci, H. S. Yamamoto, Y. Takagi, U. H. Yildiz, D. Akin, D. R. Wesemann, A. Singhal, P. L. Yang, M. L. Nibert, R. N. Fichorova, D. T. Lau, T. J. Henrich, K. M. Kaye, S. C. Schachter, D. R. Kuritzkes, L. M. Steinmetz, S. S. Gambhir, R. W. Davis, U. Demirci, *Proc. Natl. Acad. Sci. USA* **2015**, *32*, E4354–E4363.
[14] D. N. Breslauer, R. N. Maamari, N. A. Switz, W. A. Lam, D. A. Fletcher, *PloS One* **2009**, *4*, e6320.
[15] Z. J. Smith, K. Chu, A. R. Espenson, M. Rahimzadeh, A. Gryshuk, M. Molinaro, D. M. Dwyre, S. Lane, D. Matthews, S. Wachsmann-Hogiu, *PloS One* **2011**, *6*, e17150.
[16] Y. Lu, W. Shi, J. Qin, B. Lin, *Electrophoresis* **2009**, *30*, 579.
[17] P. Preechaburana, M. C. Gonzalez, A. Suska, D. Filippini, *Angew. Chem. Int. Ed. Engl.* **2012**, *51*, 11585.
[18] L. Shen, J. A. Hagen, I. Papautsky, *Lab Chip* **2012**, *12*, 4240.
[19] S. Wang, X. Zhao, I. Khimji, R. Akbas, W. Qiu, D. Edwards, D. W. Cramer, B. Ye, U. Demirci, *Lab Chip* **2011**, *11*, 3411.
[20] A. W. Martinez, S. T. Phillips, E. Carrilho, S. W. Thomas, H. Sindi, G. M. Whitesides, *Anal. Chem.* **2008**, *80*, 3699.
[21] S. Wang, R. Akbas, U. Demirci, *Methods Mol. Biol.* **2015**, *1256*, 111.
[22] S. Wang, S. Tasoglu, P. Z. Chen, M. Chen, R. Akbas, S. Wach, C. I. Ozdemir, U. A. Gurkan, F. F. Giguel, D. R. Kuritzkes, U. Demirci, *Sci. Rep.* **2014**, *4*, 3796.
[23] A. C. Sobieranski, F. Inci, H. C. Tekin, M. Yuksekkaya, E. Comunello, D. Cobra, A. von Wangenheim, U. Demirci, *Light Sci. Appl.* **2015**, doi:10.1038/lsa.2015.119.
[24] Y.-N. Wang, Y. Kang, D. Xu, C. H. Chon, L. Barnett, S. A. Kalams, D. Li, D. Li, *Lab Chip* **2008**, *8*, 309.
[25] C. Briggs, P. Harrison, S. J. Machin, *Int. J. Lab. Hematol.* **2007**, *29*, 77.
[26] X. Cheng, Y. Liu, D. Irimia, U. Demirci, L. Yang, L. Zamir, W. R. Rodríguez, M. Toner, R. Bashir, *Lab Chip* **2007**, *7*, 746–755.
[27] N. N. Watkins, S. Sridhar, X. Cheng, G. D. Chen, M. Toner, W. Rodriguez, R. Bashir, *Lab Chip* **2011**, *11*, 1437.
[28] M. T. Glynn, D. J. Kinahan, J. Ducrée, *Lab Chip* **2013**, *13*, 2731.
[29] S. Moon, U. A. Gurkan, J. Blander, W. W. Fawzi, S. Aboud, F. Mugusi, D. R. Kuritzkes, U. Demirci, *PloS One* **2011**, *6*, e21409.
[30] L. Vanjari, V. Lakshmi, V. D. Teja, M. V. S. Subbalaxmi, N. Chandra, N. P. Ede, M. Gadde, *J. Acquired Immune Defic. Syndr.* **2012**, *61*, e70.
[31] X. Ding, Z. Peng, S.-C. S. Lin, M. Geri, S. Li, P. Li, Y. Chen, M. Dao, S. Suresh, T. J. Huang, *Proc. Natl. Acad. Sci.* **2014**, *111*, 12992.
[32] A. A. Nawaz, R. H. Nissly, P. Li, Y. Chen, F. Guo, S. Li, Y. M. Shariff, A. N. Qureshi, L. Wang, T. J. Huang, *Ann. Biomed. Eng.* **2014**, *42*, 2303.
[33] S. Q. Wang, F. Inci, G. De Libero, A. Singhal, U. Demirci, *Biotechnol. Adv.* **2013**, *4*, 438–449.
[34] Y. Yang, Z. Zhang, X. Yang, J. H. Yeo, L. Jiang, D. Jiang, *J. Biomed. Opt.* **2004**, *9*, 995.
[35] M. Roy, G. Jin, D. Seo, M.-H. Nam, S. Seo, *Sens. Actuators, B* **2014**, *201*, 321.
[36] C. Grenvall, C. Antfolk, C. Z. Bisgaard, T. Laurell, *Lab Chip* **2014**, *14*, 4629.
[37] T. Songjaroen, W. Dungchai, O. Chailapakul, C. S. Henry, W. Laiwattanapaisal, *Lab Chip* **2012**, *12*, 3392.
[38] D. Heikali, D. D. Carlo, *J. Assoc. Lab. Autom.* **2010**, *15*, 319.
[39] D. Huh, W. Gu, Y. Kamotani, J. B. Grotberg, S. Takayama, *Physiol. Meas.* **2005**, *26*, R73.
[40] S. Tasoglu, C. H. Yu, H. I. Gungordu, S. Guven, T. Vural, U. Demirci, *Nat. Commun.* **2014**, *5*, 4702.
[41] S. Tasoglu, D. Kavaz, U. A. Gurkan, S. Guven, P. Chen, R. Zheng, U. Demirci, *Adv. Mater.* **2013**, *25*, 1137.
[42] K. A. Mirica, S. T. Phillips, C. R. Mace, G. M. Whitesides, *J. Agric. Food Chem.* **2010**, *58*, 6565.
[43] K. A. Mirica, F. Ilievski, A. K. Ellerbee, S. S. Shevkoplyas, G. M. Whitesides, *Adv. Mater.* **2011**, *23*, 4134.
[44] M. R. Lockett, K. A. Mirica, C. R. Mace, R. D. Blackledge, G. M. Whitesides, *J. Forensic Sci.* **2013**, *58*, 40.
[45] D. K. Bwambok, M. M. Thuo, M. B. J. Atkinson, K. A. Mirica, N. D. Shapiro, G. M. Whitesides, *Anal. Chem.* **2013**, *85*, 8442.
[46] R. R. David, W. Inglis, *J. Appl. Phys.* **2006**, *99*, 08K101.
[47] M. J. P. van Osch, E. P. A. Vonken, M. A. Viergever, J. van der Grond, C. J. G. Bakker, *Magn. Reson. Med. Off. J. Soc. Magn. Reson. Med. Soc. Magn. Reson. Med.* **2003**, *49*, 1067.
[48] N. G. Durmus, H. C. Tekin, S. Guven, K. Sridhar, A. Arslan Yildiz, G. Calibasi, I. Ghiran, R. W. Davis, L. M. Steinmetz, U. Demirci, *Proc. Natl. Acad. Sci. USA* **2015**, *112*, E3661.
[49] K. Källander, J. K. Tibenderana, O. J. Akpogheneta, D. L. Strachan, Z. Hill, A. H. A. ten Asbroek, L. Conteh, B. R. Kirkwood, S. R. Meek, *J. Med. Internet Res.* **2013**, *15*, e17.

Received: June 25, 2015
Revised: August 11, 2015
Published online:

DOI: 10.1002/smll.201501845